Photooxidation of Hydrogen-Terminated Si(111) Surfaces Studied by Optical Second Harmonic Generation

S. A. Mitchell

Steacie Institute for Molecular Sciences, National Research Council of Canada, 100 Sussex Drive, Ottawa, Ontario K1A 0R6, Canada

Received: February 21, 2003; In Final Form: June 13, 2003

Photooxidation of hydrogen-terminated Si(111) surfaces in air has been studied by using optical second harmonic generation (SHG) in reflection from the silicon surface. The mechanism of photooxidation induced by a mercury pen lamp is shown to involve oxygen atoms produced by 185-nm photodissociation of O_2 in the gas phase above the Si(111)−H surface. Several fundamental wavelengths were used for SHG, including two-photon resonant excitations that are characteristic of H-terminated and oxidized Si(111) surfaces. By focusing on the anisotropic part of the SHG response, the specific response of intra-bilayer Si−Si bonds was isolated. A pronounced nonmonotonic variation of the SHG signal was observed during photooxidation and also during oxidation of Si(111)−H surfaces in air in the dark. A simple model is described that relates modulations in the SHG signal with progressive oxidation of distinct layers of Si−Si bonds near the surface. An analysis suggests that inter- as well as intra-bilayer bonds are attacked by oxygen atoms at an early stage during photooxidation.

Introduction

Hydrophobic, hydrogen-terminated silicon surfaces formed by wet chemical etching in aqueous fluoride solutions have long been of interest for their remarkable passivation properties.[1] In 1990 it was demonstrated that ideally terminated, atomically flat H−Si(111)-1 × 1 surfaces were produced by etching of oxidized silicon surfaces in buffered fluoride solution with pH in the range 8−10.[2] Such Si(111)−H surfaces are passivated to a remarkable degree, with respect to both electrical activity[3,4] and chemical stability against oxidation in air.[5−8] The nearly perfect nature of the Si(111)−H surface is a result of anisotropic etching of silicon in aqueous fluoride solution, whereby broad H−Si(111)-1 × 1 terraces are exposed by a step-flow mechanism.[9] Such ideally terminated, atomically flat surfaces are attractive substrates for chemical modification with passivating or chemically functional films,[10] for potential applications in electronic devices or chemical/biochemical sensors. The ideal structure of the silicon crystal at the interface greatly simplifies the interpretation of experiments involving chemical modification of the silicon surface.

The stability of hydrogen-terminated silicon surfaces with respect to oxidation in air is an important issue that has received considerable attention.[5−8] Recently, Chidsey and co-workers[11] reported that the onset of oxidation of Si(111)−H surfaces in air is greatly accelerated by UV photoexcitation of the surface with a low-pressure mercury pen lamp ($\lambda = 254$ nm). It was suggested that UV photoexcitation produced dangling bonds on the surface by photodesorption of H-atoms, and oxidation proceeded by a radical chain mechanism. Wayner and co-workers[12] have used photooxidation of Si(111)−H with a contact photomask to prepare chemically patterned silicon surfaces. In the present work, optical second harmonic generation (SHG) is used as a surface-sensitive probe to study the initial stages of photooxidation of Si(111)−H surfaces in air. The light source used for photoirradiation is a low-pressure mercury pen lamp with major UV lines at 185 and 254 nm. It is shown that the mechanism of oxidation involves oxygen atoms produced by photolysis of molecular oxygen at 185 nm. The mechanism is thus similar to that which pertains in a conventional UV-ozone treatment.[13]

In previous work from this laboratory the application of SHG for monitoring chemical reactions of Si(111) surfaces has been described.[14−16] The SHG efficiency R_{pP} for p-polarized fundamental and second harmonic radiation can be expressed as shown in eq 1,

$$R_{pP} = \frac{I_P(2\omega)}{[I_p(\omega)]^2} = |A_{pP} + B_{pP}\cos(3\phi)|^2 \qquad (1)$$

where $I_p(\omega)$ and $I_P(2\omega)$ are irradiances of the fundamental and second harmonic radiation, ϕ is an angle of rotation of the silicon crystal about the (111) surface normal, and A_{pP} and B_{pP} are parameters that are related to nonlinear susceptibilities of the silicon surface as described in detail by Sipe and co-workers.[17] A similar expression applies for p-polarized fundamental and S-polarized second harmonic radiation, except in this case there is no isotropic contribution, i.e., $A_{pS} = 0$.

$$R_{pS} = \frac{I_S(2\omega)}{[I_p(\omega)]^2} = |B_{pS}\sin(3\phi)|^2 \qquad (2)$$

Note that lower (upper) case letters are used to designate polarization states of the fundamental (second harmonic) radiation. In general the isotropic A and anisotropic B parameters in eqs 1 and 2 are complex quantities. Their dispersion with the fundamental frequency near $\hbar\omega \sim 1.7$ eV reflects, in a complex manner, the electronic structure of the interface.[18] In Figure 1 are shown spectra of $|B_{pS}|^2$ for Si(111) surfaces with hydrogen termination and with a native oxide film (denoted Si(111)-ox), as reported previously.[15] Note that these surfaces

10.1021/jp0344489 CCC: $25.00 Published 2003 by the American Chemical Society
Published on Web 07/23/2003

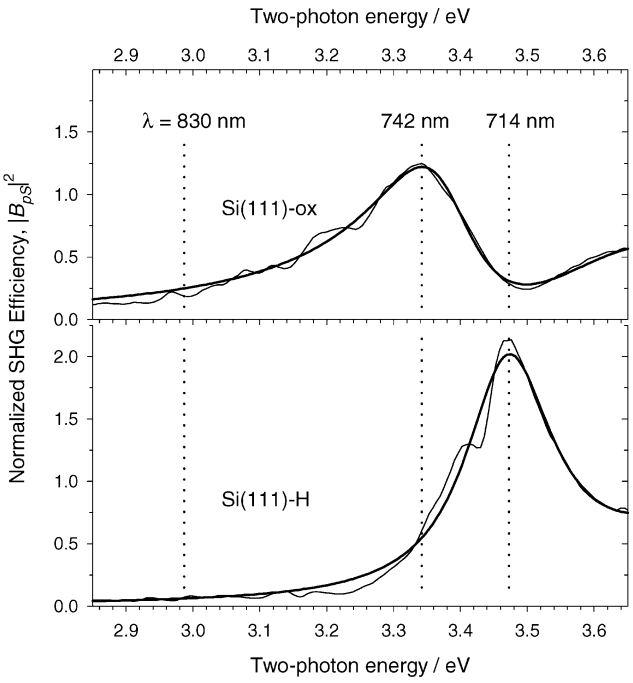

Figure 1. Second harmonic spectra showing characteristic resonances of H-terminated and native-oxide Si(111) surfaces, as reported in ref 15. The spectra show the variation of the anisotropic response $|B_{pS}|^2$ with the two-photon energy of the fundamental radiation. SHG efficiency has been normalized with respect to the second harmonic reflection from a *z*-cut quartz crystal. Several fundamental wavelengths used in this work are indicated.

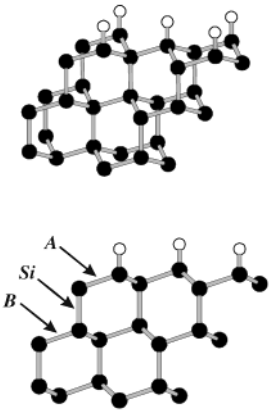

Figure 2. Structure of H−Si(111)-1 × 1 surface, showing the perspective view (top) and the side view (from the [01$\bar{1}$] direction). Open circles represent H atoms. The side view shows the positions of the first-layer intra-bilayer bonds (*A*), the first-layer inter-bilayer bonds (*Si*), and the second-layer intra-bilayer bonds (*B*). Intra-bilayer bonds have 3-fold symmetry with respect to the surface normal.

show distinct spectra, which indicates that SHG may be used to monitor the progress of oxidation of Si(111)−H surfaces. In this work several fundamental wavelengths were used for this purpose and are indicated in Figure 1.

An important feature of the anisotropic SHG response $|B_{pS}|$ is its specific association with Si−Si back-bonds in the topmost layers of the Si(111) surface. Here we are disregarding the contribution from the bulk, electric-quadrupole response of silicon,[17] which is justified in view of the pronounced sensitivity of the SHG response to the chemical state of the surface (Figure 1). The structure of a Si(111) surface is illustrated in Figure 2. Whereas the anisotropic response $|B_{pS}|$ (or $|B_{pP}|$) is specifically associated with *intra*-bilayer Si−Si back-bonds, with 3-fold symmetry with respect to the surface normal, the isotropic response $|A_{pP}|$ includes, in principle, contributions from all of the bonds in the surface region. This includes both *intra*-bilayer and *inter*-bilayer Si−Si bonds and also the bonds between the topmost Si atoms and H atoms in the case of H-termination or O atoms in the case of Si-ox surfaces. Such a simplified interpretation of SHG in terms of contributions from individual chemical bonds follows from the view that these bonds are the fundamental polarizable units present at the interface. This view is well established in the literature[18−21] and is most useful for developing a qualitative understanding of the microscopic origin of the nonlinear response.

The polarizable bond viewpoint is used in this work to interpret changes in the SHG response during the early stages of oxidation of Si(111)−H surfaces. The focus is on the anisotropic response $|B_{pS}|$, so attention is directed to the subset of bonds near the interface comprised exclusively of *intra*-bilayer Si−Si back-bonds. A further simplification is achieved by considering that the SHG response reflects an acentric character of the Si−Si bonds. In the bulk of the silicon crystal the Si−Si bonds are centrosymmetric, and therefore cannot contribute to SHG according to the rule that SHG is prohibited in media with inversion symmetry.[22] However, if one of the Si atoms of the Si−Si bond is also bonded to a foreign atom, such as H or O, then the bond becomes acentric and may contribute to the SHG response. In this way the anisotropic SHG response is associated with a subset of Si−Si bonds that is structurally distinct in the spatial arrangement of the surface layers and also distinct in terms of the local chemical environment. Such a specificity allows for interpretation of changes in SHG efficiency during oxidation of the surface in terms of microscopic aspects of the chemical reaction mechanism.

Experimental Section

Polished Si(111) wafers were supplied by Virginia Semiconductor, Inc. n-type (1−3 Ω·cm), p-type (5 Ω·cm), or n+ (0.0025 Ω·cm) wafers were cut into rhombus-shaped pieces with included angles of 60° and 120° and with a side length of 17 mm. Hydrogen-terminated Si(111) surfaces were prepared by first sonicating the silicon crystal in Milli-Q water and then cleaning in 1:3 H_2O_2 (30%):H_2SO_4 (concentrated) at 100 °C for 30 min. The hydrophilic crystal was thoroughly rinsed with Milli-Q water and then placed in argon-deaerated ammonium fluoride (40%) for 15 min. The hydrogen-terminated crystal was then dipped in argon-deaerated Milli-Q water for several seconds and dried under a stream of inert gas. All chemicals were clean room grade supplied by Amplex.

The experimental arrangement for SHG studies of chemically modified Si(111) surfaces has been described previously.[16] Laser pulses from a femtosecond optical parametric amplifier (Topas, supplied by Quantronix) were focused on the sample by using a 50 cm focal length lens and with the angle of incidence 45°. The reflected second harmonic was isolated by using a Pellin-Broca prism and colored glass filters and detected with a photomultiplier tube and boxcar amplifier. With the pulse energy ∼2 μJ, repetition rate 1 kHz, and focal spot diameter ∼0.3 mm (measured by translation of a knife edge across the beam waist), the fluence on the sample was ∼3 mJ/cm^2 and the average irradiance was ∼3 W/cm^2. The pulse duration was ∼100 fs. In all experiments a reference SHG signal from a quartz plate was measured simultaneously with the SHG signal from the sample. In addition, all SHG measurements were normalized to a signal that was recorded when a *z*-cut quartz wedge was substituted in the sample position.[16] SHG was studied for samples exposed

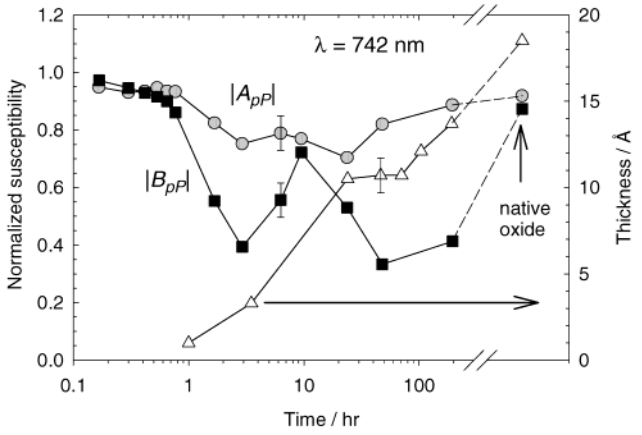

Figure 3. Variation of isotropic and anisotropic nonlinear susceptibilities during oxidation of a freshly prepared Si(111)−H surface in laboratory air, for the fundamental wavelength $\lambda = 742$ nm. The extent of oxidation is shown by the oxide film thickness as measured by ellipsometry. Also shown are results for a Si(111) surface with a native oxide film.

to laboratory air (22 °C, 25−35% relative humidity) and controlled gaseous ambients at atmospheric pressure. The ambient was controlled by optionally directing a gentle flow (∼3 L/min) of dry nitrogen (boil-off from liquid nitrogen reservoir) onto the surface of the sample.

The light source used for photooxidation of the silicon surface was a mercury pen lamp supplied by Oriel (model 6035), with major UV lines at 254 and 185 nm. The irradiance at these wavelengths was estimated by using a calibrated silicon photodiode (UDT Sensors model UV-100) and filters (Schott WG225, WG280) to isolate the 254-nm line: 2×10^{-4} W/cm^2 at 254 nm and 1×10^{-5} W/cm^2 at 185 nm, measured at a distance of 10 cm from the pen lamp. Additional studies were performed with a KrF excimer laser with $\lambda = 248$ nm (Lumonics) and a 100-W mercury arc lamp (Oriel model 6281) together with a 10 cm focal length monochromator to select the photolysis wavelength (fwhm ∼ 10 nm).

Oxidized Si(111) surfaces were characterized by X-ray photoelectron spectroscopy (XPS) and ellipsometry. XPS measurements were performed with a PHI 5500 system with monochromatic Al Kα_1 photons at 45° incidence and with a variable takeoff angle. Samples were transported to the XPS instrument under dry nitrogen and loaded in the analysis chamber within 20 min of their preparation. Oxide film thickness was measured from Si2p photoelecton intensities as described by Iwata and Ishizaka.[23] In addition, the film thickness was measured by ellipsometry, using a Gaertner model L116 S ellipsometer with a HeNe laser and an angle of incidence of 70°. $n = 1.46$ was used for the oxide film and $n = 3.85$ and $k = 0.02$ were used for the silicon substrate.

Results and Discussion

A. Oxidation of Si(111)−H in Air: Effect on SHG. In Figure 3 are shown results of rotational anisotropy measurements (according to eq 1) on Si(111)−H surfaces in air at room temperature, for the fundamental wavelength $\lambda = 742$ nm. The measurements were repeated at intervals over a period of ∼8 days, during which time significant oxidation of the surface occurred. The extent of oxidation is shown in Figure 3 by the results of ellipsometric measurements of the oxide film thickness. Also shown in Figure 3 are measured SHG parameters and ellipsometric film thickness for a native oxide film on the same substrate material. Similar behavior was observed during oxidation of Si(111)−H on n-type and p-type silicon substrates. However, n+ substrates showed distinctly different SHG efficiency starting at the earliest stages of oxidation. This is due to the importance of electric field induced SHG (EFISH) for oxidized surfaces of n+ substrates only and not for n-type or p-type substrates.[14] All of the results presented in this work were obtained for n-type silicon substrates.

Measurements of the type shown in Figure 3 were performed repeatedly, using the fundamental wavelength $\lambda = 714$ nm as well as 742 nm. It was found that the variation of isotropic $|A_{pP}|$ and anisotropic $|B_{pP}|$ SHG parameters with oxide film thickness was reproducible, but the rate of oxidation of Si(111)−H in air was remarkably variable. We were not able to ascertain the cause of this variability, and it was concluded that the preparation and handling conditions that we used (being typical of a chemical laboratory) were inadequate for a systematic study of this effect. Control experiments indicated that the laser irradiation that was used for observing SHG was not a significant influence on the stability of the Si(111)−H surface. Uosaki and co-workers[24] have shown that Si(111)−H surfaces are unstable with respect to prolonged visible-wavelength laser irradiation in laboratory air.

A significant feature of the results in Figure 3 for the fundamental wavelength $\lambda = 742$ nm is the large, nonmonotonic variation of the anisotropic response $|B_{pP}|$ during the early stages of oxide film growth. This is in contrast with the isotropic response $|A_{pP}|$, which shows a relatively small variation. A similar effect was reported previously for the fundamental wavelength $\lambda = 714$ nm,[15] i.e., a pronounced, nonmonotonic variation of $|B_{pP}|$ and a monotonic variation of $|A_{pP}|$ during the early stages of oxidation of Si(111)−H. Qualitatively similar effects were observed in the present study during photooxidation of the Si(111)−H surface. Photooxidation in laboratory air was induced by a mercury pen lamp positioned 10 cm from the silicon surface. Figure 4 shows the variation of the anisotropic SHG response $|B_{pS}|$ measured in situ during irradiation of the surface with the pen lamp, for the fundamental wavelengths $\lambda = 714$, 742, and 830 nm. Also shown in Figure 4 is the variation of the ellipsometric film thickness as measured for the same photoirradiation conditions for a separate Si(111)−H sample. In contrast with the nonmonotonic variation of $|B_{pS}|$ for $\lambda = 714$, 742, and 830 nm shown in Figure 4, in all cases the isotropic response $|A_{pP}|$ showed a monotonic variation (not shown in Figure 4) during the initial stages of photooxidation of the Si(111)−H surface.

It should be noted that the stability of the Si(111)−H surface in air under the photoexcitation conditions used for monitoring SHG was such that only insignificant oxidation occurred in the absence of UV illumination by the mercury pen lamp. This is illustrated in Figure 4 for the case of the fundamental wavelength $\lambda = 714$ nm. It is seen that the rate of photooxidation induced by UV illumination with the pen lamp greatly exceeded the rate of oxidation in air under laser irradiation alone.

Our results indicate that the variation of isotropic and anisotropic contributions to the SHG response is similar for oxidation of Si(111)−H with and without auxiliary photoexcitation of the surface. The variation of $|B_{pS}|$ (or $|B_{pP}|$) shown in Figures 3 and 4 is consistent with previously reported tabulations of normalized SHG efficiencies for H-terminated and native oxide Si(111) surfaces[14−16] (see also Figure 1). For the fundamental wavelength $\lambda = 714$ nm, the SHG efficiency of Si(111)−H is significantly greater than that of the native oxide, so one expects a decrease in SHG efficiency during oxidation. Conversely, a significant increase is expected for $\lambda = 830$ nm,

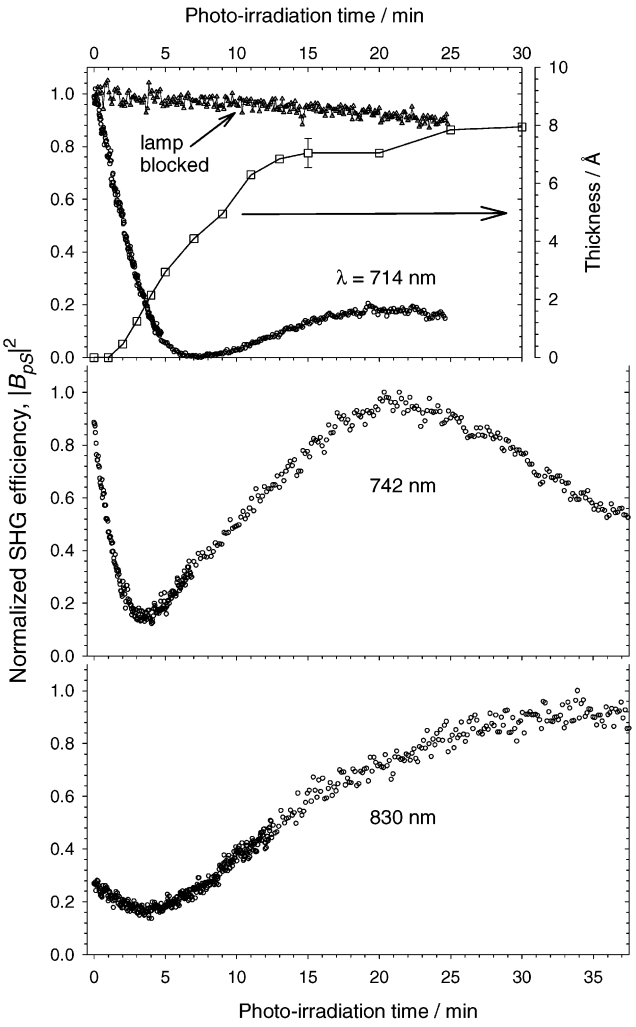

Figure 4. Variation of anisotropic SHG response $|B_{pS}|^2$ during photooxidation of freshly prepared Si(111)−H surfaces in laboratory air, for the fundamental wavelengths $\lambda = 714$, 742, and 830 nm. The mercury pen lamp was positioned 10 cm from the silicon surface. SHG efficiency has been normalized such that the maximum value is unity in each trace. The top panel shows the variation of the oxide film thickness during photooxidation of a separate sample under identical conditions, as measured by ellipsometry. Also shown in the top panel is the variation of the SHG response for a separate sample when the illumination of the mercury pen lamp was blocked from the surface.

while for $\lambda = 742$ nm a smaller overall change in SHG efficiency is expected upon oxidation. These effects are present in the results in Figure 4, considering specifically the trends for photoirradiation times less than 20 min. However, the pronounced nonmonotonic behavior of $|B_{pS}|$ is unexpected. The significance of this behavior is discussed in Section C.

B. Kinetics and Mechanism of Photooxidation of Si(111)−H. The initial rate of photooxidation of Si(111)−H in laboratory air was studied by monitoring the anisotropic SHG response $|B_{pS}|$ for the fundamental wavelength $\lambda = 714$ nm. As shown in Figure 1, this corresponds with a maximum response for Si(111)−H and a relatively small response for the native oxide. The signal decreased nearly to zero during the early stages of photooxidation (Figure 4, $\lambda = 714$ nm). In Figure 5 are shown several traces that illustrate the time dependence of $|B_{pS}|$ during photoirradiation of freshly prepared Si(111)−H surfaces with the mercury pen lamp under various conditions. In traces B and C the lamp was moved closer to the surface compared with trace A, such that the irradiance of the lamp at the sample

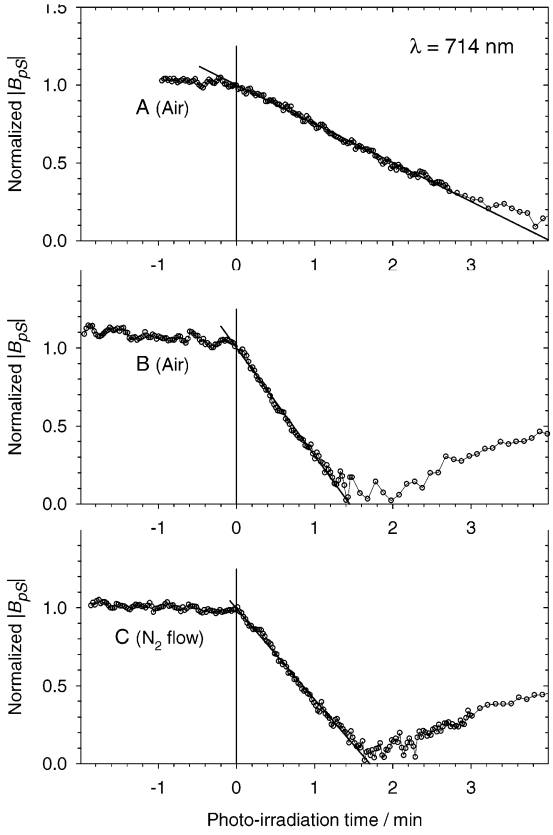

Figure 5. Kinetic traces showing variation of the anisotropic SHG response $|B_{pS}|$ during photoirradiation of freshly prepared Si(111)−H surfaces with a mercury pen lamp. The fundamental wavelength was $\lambda = 714$ nm. Zero on the time axis indicates the point at which the surface was exposed to unfiltered radiation from the pen lamp. At negative times the radiation was filtered to remove the far-UV (185 nm) mercury resonance line. Straight lines through the data points show linear fits to the early parts of the curves. A: Lamp positioned 10 cm from the surface in laboratory air. B: Lamp positioned 7.1 cm from the surface in laboratory air. C: Lamp positioned 7.1 cm from the surface in a crude N_2 purge.

position increased by a factor of 2. This caused the decay rate of the signal to increase by approximately the same factor, as would be expected for a photochemical process induced by the pen lamp.

The kinetic traces in Figure 5 illustrate two important observations that reveal the mechanism of the photooxidation process. First, photooxidation was induced not by the main resonance line of the mercury pen lamp at 254 nm but by the far-UV line at 185 nm. This was proven by using a transmission filter (Schott WG225) that blocked the far-UV line but transmitted the 254 nm line. The traces in Figure 5 show the effect of the filter. The beginning of each trace corresponds with the time of the initial exposure of the freshly prepared Si(111)−H surface to the illumination of the pen lamp, including the far-UV blocking filter. The zero of the time axis indicates when the filter was removed and the sample was exposed to the full spectrum of the lamp including the far-UV line at 185 nm. It is clear that the onset of photooxidation corresponds with exposure of the sample to the far-UV radiation. The relative ineffectiveness of 254-nm radiation was confirmed by experiments with a mercury arc lamp in combination with a monochromator (irradiance ~1 mW/cm^2 at 254 nm with fwhm 10 nm) and also a KrF excimer laser (248 nm, 0.5 mJ/pulse, 10 mW/cm^2). In comparison, the irradiance of the pen lamp at 254 nm was ~0.2 mW/cm^2 at the sample position.

The second observation illustrated in Figure 5 concerns the effect of the ambient atmosphere on the rate of photooxidation of the Si(111)−H surface. For traces A and B the ambient was laboratory air, while for trace C a continuous flow (∼3 L/min) of dry nitrogen gas was passed over the Si(111)−H surface. The effect of this treatment was to reduce the partial pressure of oxygen above the sample by an estimated factor of ∼0.01. It was at first surprising that such a treatment caused only a minor reduction in the rate of photooxidation, as shown in Figure 5. This shows that the rate of photooxidation was very weakly dependent on the pressure of O_2 above the sample, for O_2 pressures in the range investigated. As shown below, this result is consistent with a mechanism involving attack on the surface by oxygen atoms produced by UV photolysis of O_2.

Consider the gas-phase processes R1 and R2 with effective first-order rate coefficient k_1 and second-order rate coefficient k_2, respectively.

$$O_2 + h\nu(185\ \text{nm}) \rightarrow 2O \qquad \text{(R1)}$$

$$O + O_2 \rightarrow O_3 \qquad \text{(R2)}$$

The time dependence of the concentration of O atoms is given by eq 3.

$$[O] = \frac{2k_1}{k_2}\{1 - \exp(-k_2[O_2]t)\} \qquad (3)$$

A steady-state concentration of O atoms $[O]_{ss} = 2k_1/k_2$ is established in the gas phase with a time constant $\tau = 1/k_2[O_2]$. Note that $[O]_{ss}$ is independent of the pressure of O_2. A simple estimate of the rate of photooxidation is obtained by considering the flux Z of O atoms on the Si(111)−H surface due to a steady-state concentration $[O]_{ss}$ in the gas-phase just above the surface. The flux is given by eq 4,[25] where $\bar{c}$ is the average speed of O atoms at room temperature. The irradiance of the pen lamp at

$$Z = {}^1/_4[O]_{ss}\bar{c} \qquad (4)$$

185 nm at a distance of 10 cm was estimated as 1×10^{-5} W/cm^2 or 1×10^{13} cm^{-2} s^{-1}, with a large uncertainty in the range of a factor of 2 or 3. By using literature values of rate parameters including photochemical data from ref 26, the steady-state concentration of O atoms was estimated as $[O]_{ss} \sim 3 \times 10^7$ cm^{-3}, and the time constant for achieving steady-state conditions is $\tau \sim 10^{-5}$ s for the case of laboratory air and $\tau \sim 2$ s for a partial pressure of O_2 as low as 10^{-3} Torr.[27] This shows that the steady state was established effectively instantaneously in this work. The flux of O atoms on the surface was $Z \sim 4.5 \times 10^{11}$ cm^{-2} s^{-1}, from eq 4. In comparison, the density of H atoms on the Si(111)−H surface is $N_0 = 7.8 \times 10^{14}$ cm^{-2}. Thus, the integrated flux of O atoms attained the value N_0 in ∼30 min, which is similar to the time scale for formation of an oxide film in Figure 4 (from ellipsometry measurements). Such a correlation is expected since the sticking coefficient of O atoms on Si(111)−H surfaces is near unity.[28,29]

To quantify the rate of photooxidation the following simplified model is used. The rate of change of the coverage of O atoms on the surface is given by eq 5, where $\Theta = N/N_0$ with N the surface density of adsorbed O atoms. Θ_S is the value of Θ

$$\frac{d\Theta}{dt} = \frac{Z}{N_0}\left(1 - \frac{\Theta}{\Theta_S}\right) \qquad (5)$$

at saturation coverage. In this model the sticking coefficient of O atoms is taken as unity.[29] The nonlinear susceptibility χ is assumed to be related to the coverage as shown in eq 6, where χ_0 is the nonlinear susceptibility of the bare surface.[30] The

$$\chi = \chi_0(1 - \alpha\Theta) \qquad (6)$$

parameter α should generally be larger than unity; its interpretation is discussed in section C below. From eqs 5 and 6, the time dependence of the nonlinear susceptibility is given by eq 7. If $\alpha = 1$ in eq 7 then a simple exponential decay results,

$$\chi = \chi_0\{1 - \alpha\Theta_S + \alpha\Theta_S \exp(-Zt/\Theta_S N_0)\} \qquad (7)$$

since Θ_S can be taken as unity by a change in the definition of Θ. On the other hand, if α is significantly larger than unity then a distinctly nonexponential decay results. In either case, expanding the exponential in eq 7 leads to a linear time dependence as shown in eq 8. This result is valid provided the

$$\chi = \chi_0\{1 - (\alpha Z/N_0)t\} \qquad (8)$$

argument of the exponential in eq 7 is small compared to unity, which pertains at low fractional coverage of $\Theta_S N_0$ adsorption sites. An important feature of the $\alpha > 1$ case of eq 7 is that the approximation leading to eq 8 may remain valid even as χ/χ_0 approaches zero. This is not the case when $\alpha = 1$, because in this case the decay of χ/χ_0 is a simple exponential. The results shown in Figure 5 for the fundamental wavelength $\lambda = 714$ nm are consistent with the linear time dependence shown in eq 8. From the slope of a linear fit to the data the quantity $\alpha Z/N_0$ was evaluated as 2.9×10^{-3} s^{-1}, and thus $\alpha Z = 2.3 \times 10^{12}$ cm^{-2} s^{-1}, using $N_0 = 7.8 \times 10^{14}$ cm^{-2}. This compares with $Z \sim 4.5 \times 10^{11}$ cm^{-2} s^{-1} estimated from eq 4. These results are consistent and suggest $\alpha \sim 5$. Note, however, that the magnitude of α is not well-determined considering the uncertainty of the estimate of Z from eq 4.

An independent estimate of the growth rate of the oxide was obtained from measurements of the oxide film thickness. In addition to the ellipsometry measurements shown in Figure 4, several samples were analyzed by using X-ray photoelectron spectroscopy (XPS). It was concluded that the ellipsometric measurements of oxide film thickness were systematically high. This conclusion is consistent with results of other workers using similar methods.[23] The XPS results indicated that the oxide film thickness following ∼30 min of photooxidation in laboratory air was ∼4 Å, rather than 8 Å as indicated from the ellipsometry results shown in Figure 4. A straightforward calculation using the density of SiO_2 (2.65 g/cm^3)[31] then indicates that the flux of O atoms on the surface was $Z \sim 1.2 \times 10^{12}$ cm^{-2} s^{-1}, assuming unit sticking probability. This figure is consistent with the estimates from eq 4 ($Z \sim 4.5 \times 10^{11}$) and from the analysis of kinetic data using eq 8 ($\alpha Z = 2.3 \times 10^{12}$). The proposed mechanism of the photooxidation process is therefore confirmed.

C. Interpretation of SHG Response: Polarizable Bond Model. As shown in Figure 4, during the early stages of photooxidation of Si(111)−H the anisotropic response $|B_{pS}|$ for the fundamental wavelength $\lambda = 742$ nm decreased significantly faster than that for $\lambda = 714$ nm. In both cases a significant increase in the response occurred after the initial decrease, with the increase being more pronounced for $\lambda = 742$ nm than for $\lambda = 714$ nm. A possible explanation for the relatively fast initial decrease for $\lambda = 742$ nm is that the component of the response that increased was out-of-phase with the component that initially decreased. If the "increasing" contribution grew concurrently with the initial decay of the "decreasing" contribution, then

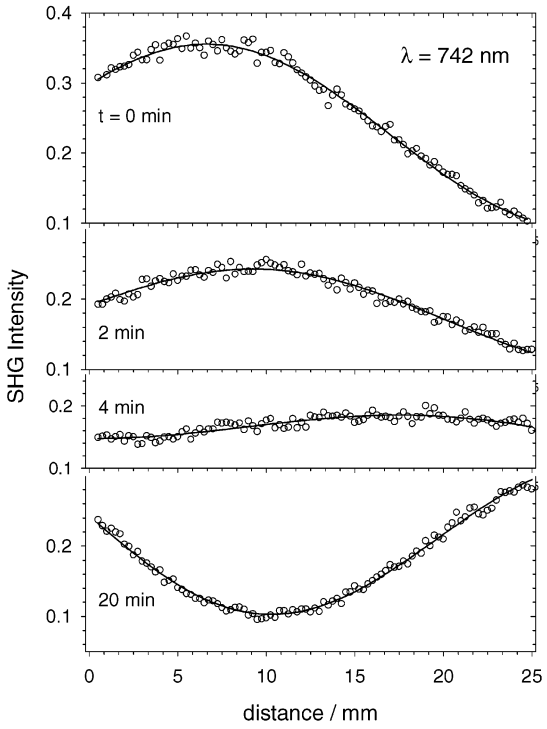

Figure 6. Measurement of the relative phase of anisotropic SHG response during photooxidation of Si(111)−H surface in air, for the fundamental wavelength $\lambda = 742$ nm. The photoirradiation times are indicated. Solid lines show fits of the data to eq 9.

interference between these components with opposite phase would result in an accelerated initial decrease. Thus, the difference in behavior between $\lambda = 714$ and 742 nm could arise from different phase relationships as well as relative amplitudes of the "increasing" and "decreasing" components.

To investigate this question, measurements of the relative phase of the SHG response $|B_{pS}|$ were performed by using the approach described by Kemnitz et al.[32] A thin ($\sim$100 μm) *z*-cut quartz plate was inserted in the beam reflected from the Si(111)−H surface so as to produce an auxiliary SHG signal. Displacement of the quartz plate in the direction parallel to the reflected beam caused the phase of the auxiliary SHG signal to change relative to the phase of the signal from the sample. The displacement therefore produced a modulation of the observed SHG signal, due to interference of the second harmonic fields from the sample and quartz plate as described by eq 9. Here *S*

$$S = E_1^2 + E_2^2 + 2E_1E_2\cos(\Delta\phi) \tag{9}$$

is proportional to the observed signal, E_1 and E_2 are the magnitudes of the second harmonic fields from the sample and quartz plate, respectively, and $\Delta\phi = |\phi_1 - \phi_2|$ is the relative phase of the fields. The variation of the relative phase with the displacement *d* of the quartz plate is given by eq 10, where $\Delta\phi_o$ is the relative phase at a fixed value of the displacement, λ is the fundamental wavelength, and n_ω ($n_{2\omega}$) is the index of refraction of air at the fundamental (second harmonic) wavelength.[32]

$$\Delta\phi = \Delta\phi_o + \frac{4\pi d}{\lambda}(n_{2\omega} - n_\omega) \tag{10}$$

Figure 6 shows data for relative phase measurements for a freshly prepared Si(111)−H surface and for the same surface following photoirradiation with the mercury pen lamp for the

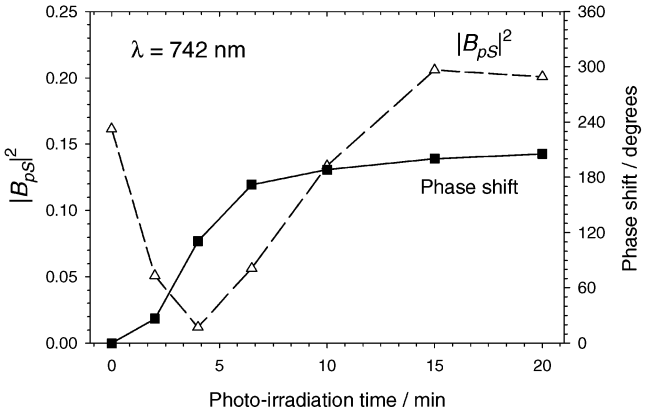

Figure 7. Variation of the relative phase of anisotropic SHG response during photooxidation of Si(111)−H surface in air, for the fundamental wavelength $\lambda = 742$ nm. Also shown is the variation of the magnitude of the SHG response as obtained from fits to the data as in Figure 6. Data points are connected by straight lines.

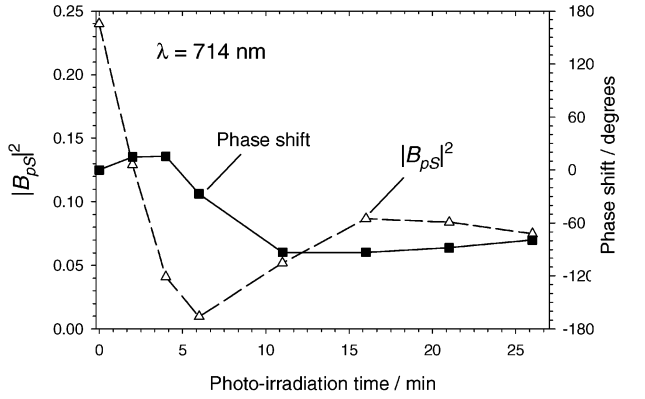

Figure 8. Variation of the relative phase of anisotropic SHG response during photooxidation of Si(111)−H surface in air, for the fundamental wavelength $\lambda = 714$ nm. Also shown is the variation of the magnitude of the SHG response as obtained from fits to the data as in Figure 6. Data points are connected by straight lines.

indicated times. The fundamental wavelength was $\lambda = 742$ nm and the SHG signal from Si(111)−H corresponded to $|B_{pS}|^2$. Similar measurements were performed for the fundamental wavelength $\lambda = 714$ nm. The data were fit to eq 9 by using eq 10 with $(4\pi/\lambda)(n_{2\omega} - n_\omega) = 0.174$ mm^{-1} for $\lambda = 714$ nm and 0.155 mm^{-1} for $\lambda = 742$ nm.[31] The parameters obtained from the fits were E_1, E_2, and $\Delta\phi_o$. To obtain reliable results it was necessary to include in the fits the variation of the magnitude of the second harmonic field from the quartz plate with the displacement *d*, which was present due to divergence of the fundamental beam over the range of *d* (25 mm, see Figure 6). The reliability of this procedure was confirmed by measurements on Si(111)−H, Si(111)-ox, and *z*-cut quartz surfaces. As expected, in all cases 180(±5)° phase shifts were observed for the $|B_{pS}|$ SHG response upon azimuthal rotation of the surface in 60° increments.[33]

The parameter E_1 is proportional to $|B_{pS}|$, and thus the measurements show the correlation of the magnitude $|B_{pS}|$ with the relative phase of the response during the early stages of oxidation of the Si(111)−H surface. The results obtained for E_1 and $\Delta\phi_o$ are shown in Figures 7 and 8 for $\lambda = 742$ and 714 nm, respectively. In both figures the relative phase was set to zero for the freshly prepared Si(111)−H surface, since only changes in the relative phase are significant. The fitted parameter E_1 is given as E_1^2, to facilitate comparison with the results in

Figure 4. As expected, the results for E_1^2 shown in Figures 7 and 8 reproduce the variation of the anisotropic response $|B_{pS}|^2$ during photooxidation, as displayed in Figure 4. It is seen that during the initial decrease and subsequent increase of the $|B_{pS}|^2$ SHG signal caused by photooxidation of the Si(111)−H surface, the $|B_{pS}|$ response for λ =742 nm underwent an approximately 180° phase shift, while that for λ = 714 nm was ∼90°. This is consistent with the interpretation of the relatively fast initial decrease of the SHG signal for λ = 742 nm as arising from interference between "increasing" and "decreasing" components of opposite phase, as described above.

To investigate further this interpretation of the SHG results, the following model is used. As explained in the Introduction, the anisotropic SHG response $|B_{pS}|$ is specifically associated with *intra*-bilayer Si−Si back-bonds in the topmost layers of the silicon surface, with 3-fold symmetry with respect to the surface normal (Figure 2). In the following the term "back-bond" is used specifically to indicate *intra*-bilayer Si−Si bonds. Two contributions to the $|B_{pS}|$ response are considered in the model, corresponding to the "decreasing" and "increasing" components described above. These are associated with the back-bonds in the first and second bilayers, denoted *A* and *B* in Figure 2. A key point of the model is that the back-bonds are considered to be active with respect to SHG only if the normally oriented *inter*-bilayer bonds above the bilayer are heteropolar. A justification for this hypothesis may be given in terms of the rule that prohibits SHG in the electric-dipole approximation in the case where the nonlinear medium has inversion symmetry. In a polarizable bond model,[21] the Si−Si back-bonds are considered as the fundamental polarizable units that comprise the nonlinear medium. These bonds are centrosymmetric unless one of the Si atoms is also bonded to a foreign atom, in which case the back-bonds become acentric due to electronegativity perturbation.[16]

The topmost bilayer of the clean Si(111)−H surface is terminated by H atoms, so the normally oriented bonds are heteropolar (Si−H) and the first-layer back-bonds are active with respect to SHG. The first inter-bilayer bonds (*Si* in Figure 2) are homopolar, and thus the second bilayer back-bonds (*B* in Figure 2) are inactive with respect to SHG in this model. However, the bonds to the second bilayer may become heteropolar if O atoms are inserted in the inter-bilayer bonds. Thus, the back-bonds *B* in Figure 2 contribute to SHG only upon oxidation of the first inter-bilayer bonds. These second layer back-bonds are associated with the component of the $|B_{pS}|$ response that increased during the early stages of photooxidation.

In this work an attempt has been made to quantify the above model to further explore the interpretation of the SHG results in terms of reactions of distinct layers of Si−Si bonds. Many previous studies have addressed the mechanism of oxidation of H-terminated silicon surfaces by thermal oxidation, reaction with O atoms, and air-oxidation at room temperature.[5−8,28,29,34,35] An issue of importance in this work is the growth mode of the oxide film by a layer-by-layer mechanism or a vertical mode involving oxide nuclei that penetrate several layers. It is known that O atoms react with H-terminated silicon surfaces with unit sticking probability, and evidence for a sequential, layer-by-layer oxidation mechanism has been described for O atoms reacting with Si(111)[34] and Si(100)[29] surfaces. In the following a simple analysis is described that provides a more detailed interpretation of the nonmonotonic variation of the anisotropic SHG response during photooxidation of Si(111)−H.

The scheme of photooxidation of Si(111)−H can be represented by reactions R3−R5.

$$A + \mathrm{O} \rightarrow \mathrm{ox} \tag{R3}$$

$$Si + \mathrm{O} \rightarrow \mathrm{B}^* \tag{R4}$$

$$B^* + \mathrm{O} \rightarrow \mathrm{ox} \tag{R5}$$

A and *Si* represent first-layer back-bonds and inter-bilayer bonds, respectively (as indicated in Figure 2), O represents atomic oxygen, and ox represents a back-bond with an inserted O atom. The species *B** represents the second-layer back-bonds in the special case where an O atom has been inserted in the inter-bilayer bond *Si*, thus rendering the back-bonds *B* active with respect to SHG. In this model the SHG response comes only from *A* and *B** back-bonds, and is thus composed of an initially decreasing component (*A*) and an increasing component (*B**). At longer times the component *B** decreases due to attack of O on second-layer back-bonds (reaction R5).

The surface coverage of species *A* is described in terms of a surface density [*A*], and the SHG response is taken to be proportional to [*A*]. The building block for species *A* is the set of three, trigonally disposed back-bonds connected to a Si atom in the topmost layer of the surface. This unit will be denoted ≡Si−H. It is supposed that several contiguous ≡Si−H units are needed to give an additive contribution associated with *A*, where the net effect of many such contributions is the $|B_{pS}|$ response that is characteristic of Si(111)−H. In the limit of low coverage of O atoms, the surface density of *A* is described by eq 11, where N_0 is the density of ≡Si−H for the clean surface and *N* is the surface density of adsorbed O atoms. The quantity

$$[A] = \frac{N_0}{\alpha} - N \tag{11}$$

α is a parameter that relates the surface density of *A* on the clean Si(111)−H surface to the density of ≡Si−H. This definition of species *A* implies that removal of a single back-bond by reaction with O has the effect of eliminating the contributions of several ≡Si−H units from the measured SHG response. This is reasonable because the reaction perturbs several ≡Si−H units in the vicinity of the reaction site. The anisotropic response $|B_{pS}|$ reflects the 3-fold symmetry of a ≡Si−H unit, and the reaction is supposed to destroy this symmetry in several ≡Si−H units.

The following analysis applies in the limit of low coverage of O atoms. The surface density of species *B** is taken to be that of O atoms inserted in the inter-bilayer bonds denoted *Si* in Figure 2. The fractional coverage of the surface by species *A* and *B** is denoted f_A and f_B, respectively, as defined by eq 12 and 13, and the associated nonlinear susceptibilities are given in eq 14 and 15.

$$f_A = \alpha[A]/N_0 \tag{12}$$

$$f_B = [B^*]/N_0 \tag{13}$$

$$\chi_A = \chi_A^0 f_A \tag{14}$$

$$\chi_B = \chi_B^0 f_B \tag{15}$$

χ_A^0 and χ_B^0 refer to the nonlinear susceptibilities for unit fractional coverages f_A and f_B. Equation 14 is equivalent to eq 6, since $f_A = (1 - \alpha\Theta)$ according to eq 11 and 12. The observed SHG signal, denoted *S*, can be expressed as shown in eq 16, where $\Delta\phi$ is the relative phase of the SHG response of species

A and *B**, and $\rho = |\chi_B^0|/|\chi_A^0|$. Note that *S* is normalized such

$$S = f_A^{\,2} + \rho^2 f_B^{\,2} + 2\rho f_A f_B \cos(\Delta\phi) \qquad (16)$$

that $S = 1$ for the clean Si(111)−H surface. For a simple analysis, the relative phase in eq 16 may be approximated as $\Delta\phi \sim 90°$ for $\lambda = 714$ nm and $\Delta\phi \sim 180°$ for $\lambda = 742$ nm, as indicated by the results in Figures 7 and 8. If the ratio of nonlinear susceptibilities ρ were known, then the simplified eq 16 for $\lambda = 714$ and 742 nm could be used to deconvolute the observed SHG signal to give directly the variation of f_A and f_B during the initial stages of photooxidation of Si(111)−H.

A simple statistical model is used to predict the fractional abundance of *B** species at a Si(111) surface with a native oxide film. The statistical model has been described by Chiang and co-workers,[36] and verified by core-level photoemission measurements on thin oxide films on Si(111) surfaces. In the present notation, the model predicts $f_B = {}^1/_3$. Its application to native oxide films may not be justified, but it provides a starting point for application of eq 16. Combining $f_B = {}^1/_3$ for a native oxide film and $f_A = 1$ for Si(111)−H with previously reported measurements[15] of $|B_{pP}|$ for the same surfaces, the ratio ρ is evaluated as shown in eq 17 (using an obvious notation for the previously measured $|B_{pP}|$). Equation 17 gives $\rho = 0.76$ for λ

$$\rho = \frac{|\chi_B^0|}{|\chi_A^0|} = \frac{3|B_{pP}|_{ox}}{|B_{pP}|_H} \qquad (17)$$

$= 714$ nm and $\rho = 2.7$ for $\lambda = 742$ nm.

Eqation 16 may now be used to obtain information on the relative rates of reaction of O atoms at specific locations on the Si(111)−H surface. In the low coverage limit, insertion of O is assumed to be limited to the topmost inter- and intra-bilayer Si−Si bonds of the surface (see Figure 2). Insertion of O in Si−H bonds is not explicitly considered, since it is known that O atoms react primarily with Si−Si bonds.[28] With the simplifications described above, eq 16 may be written as $S = f_A^2 + (0.58)f_B^2$ for $\lambda = 714$ nm, and $S = f_A^2 + (7.3)f_B^2 - (5.4)f_A f_B$ for $\lambda = 742$ nm. At low coverage of O the f_B term in the expression for $\lambda = 714$ can be neglected, and thus f_A is obtained directly. This is consistent with the kinetic analysis of Section B. The quantity f_B may now be found from the data for $\lambda = 742$ nm. The results are conveniently given in terms of relative rates. The time dependence is written as $f_A \sim 1 - k_A t$ and $f_B \sim k_B t$, as appropriate for low coverage. In Section B the rate coefficient k_A was formulated as $k_A = \alpha Z/N_0$. The rate coefficient k_B can similarly be formulated as $k_B = pZ/N_0$, where *p* is the probability that O atom insertion occurs at the *inter*-bilayer position (producing *B**). The ratio of rate coefficients is then expressed as $k_B/k_A = p/\alpha$. From an analysis of kinetic data of the type shown in Figure 4, and using the simplifications described above, the ratio of rate coefficients was evaluated as $k_B/k_A \sim 0.26$. Assuming $\alpha > 1$, this implies $p > 0.26$. From a purely statistical point of view, one would expect $p = 0.25$, since this is the fraction of reaction sites of the inter-bilayer type. The result $p > 0.26$ seems unrealistic, since there is no reason to expect a preference for insertion in inter-bilayer bonds. However, considering the approximate nature of the analysis, the quantitative significance of the result is questionable. On a qualitative level, the analysis leads to the conclusion that inter-bilayer insertion occurs at an early stage in the photooxidation process. There appears to be no significant delay in the onset of inter-bilayer insertion, and a strict layer-by-layer model is not applicable.

Conclusion

In this work the application of SHG for studies of the mechanism of photooxidation of Si(111)−H surfaces has been described. Photooxidation induced by a mercury pen lamp was shown to involve reaction of oxygen atoms produced by far-UV (185 nm) photodissociation of O_2. The relatively strong 254-nm line of the mercury lamp is much less effective for photooxidation. The mechanism of photooxidation is such that the rate of oxidation is approximately independent of O_2 pressure over a broad pressure range. This is significant for photopatterning of Si(111)−H surfaces,[12] because it means that processing can be done under conditions that favor enhanced stability of Si(111)−H in the dark.

The variation of the anisotropic SHG response $|B_{pS}|$ during photooxidation has been analyzed in terms of a simple model that considers two contributions to the response, associated with first- and second-layer back-bonds of the Si(111) surface. A key feature of the model concerns the origin of the response that grows in during the early stages of photooxidation. This contribution is attributed to second-layer back-bonds that become active with respect to SHG only upon insertion of oxygen atoms in inter-bilayer bonds. The model explains modulations in the SHG response in terms of progressive reactions of distinct layers of the Si(111)−H surface. The modulations are observed during air oxidation in the dark and also during photooxidation. From a simple analysis it was concluded that there is no strong preference for attack of oxygen atoms at intra- or inter-bilayer bonds during the early stages of photooxidation. Further work is needed to confirm this conclusion and to validate the assumptions concerning the microscopic origin of the SHG response.

Acknowledgment. The author thanks John Hulse for assistance with XPS measurements, Costel Flueraru for assistance with sample preparation, and Dan Wayner for useful discussions.

References and Notes

(1) Grundner, M.; Jacob, H. *Appl. Phys. A* **1986**, *39*, 73.
(2) Higashi, G. S.; Chabal, Y. J.; Trucks, G. W.; Raghavachari, K. *Appl. Phys. Lett.* **1990**, *56*, 656.
(3) Hsu, J. W. P.; Bahr, C. C.; vom Felde, A.; Downey, S. W.; Higashi, G. S.; Cardillo, M. J. *J. Appl. Phys.* **1992**, *71*, 4983.
(4) Yablonovitch, E.; Allara, D. L.; Chang, C. C.; Gmitter, T.; Bright, T. B. *Phys. Rev. Lett.* **1986**, *57*, 249.
(5) Miura, T.; Niwano, M.; Shoji, D.; Miyamoto, N. *Appl. Surf. Sci.* **1996**, *100/101*, 454.
(6) Niwano, M.; Kageyama, J.; Kurita, K.; Kinashi, K.; Takahashi, I.; Miyamoto, N. *J. Appl. Phys.* **1994**, *76*, 2157.
(7) Neuwald, U.; Hessel, H. E.; Feltz, A.; Memmert, U.; Behm, R. J. *Appl. Phys. Lett.* **1992**, *60*, 1307.
(8) Morita, M.; Ohmi, T.; Hasegawa, E.; Kawakami, M.; Ohwada, M. *J. Appl. Phys.* **1990**, *68*, 1272.
(9) Hines, M. A. *Int. Rev. Phys. Chem.* **2001**, *20*, 645.
(10) For a recent review see: Buriak, J. M. *Chem. Rev.* **2002**, *102*, 1271.
(11) Cicero, R. L.; Linford, M. R.; Chidsey, C. E. D. *Langmuir* **2000**, *16*, 5688.
(12) Wojtyk, J. T. C.; Tomietto, M.; Boukherroub, R.; Wayner, D. D. M. *J. Am. Chem. Soc.* **2001**, *123*, 1535.
(13) Vig, J. R. *J. Vac. Sci. Technol. A* **1985**, *3*, 1027.
(14) Mitchell, S. A.; Ward, T. R.; Wayner, D. D. M.; Lopinski, G. P. *J. Phys. Chem. B* **2002**, *106*, 9873.
(15) Mitchell, S. A.; Mehendale, M.; Villeneuve, D. M.; Boukherroub, R. *Surf. Sci.* **2001**, *488*, 367.
(16) Mitchell, S. A.; Boukherroub, R.; Anderson, S. *J. Phys. Chem. B* **2000**, *104*, 7668.
(17) Sipe, J. E.; Moss, D. J.; van Driel, H. M. *Phys. Rev. B* **1987**, *35*, 1129.
(18) Downer, M. C.; Mendoza, B. S.; Gavrilenko, V. I. *Surf. Interface Anal.* **2001**, *31*, 966.
(19) Powell, G. D.; Wang, J.-F.; Aspnes, D. E. *Phys. Rev. B* **2002**, *65*, 205320.

(20) Mendoza, B. S.; Mochán, W. L. *Phys. Rev. B* **1997**, *55*, 2489.
(21) Patterson, C. H.; Weaire, D.; McGilp, J. F. *J. Phys.: Condens. Matter* **1992**, *4*, 4017.
(22) Shen, Y. R. *Annu. Rev. Phys. Chem.* **1989**, *40*, 327.
(23) Iwata, S.; Ishizaka, A. *J. Appl. Phys.* **1996**, *79*, 6653.
(24) Shen, Y.; Saito, T.; Hihonyanagi, S.; Uosaki, K.; Miranda, P. B.; Kim, D.; Shen, Y. R. *Surf. Sci.* **2001**, *476*, 121.
(25) Moore, W. J. *Physical Chemistry*, 4th ed.; Prentice Hall: London, UK, 1972; p 133.
(26) Baulch, D. L.; Cox, R. A.; Hampson, R. F., Jr.; Kerr, J. A.; Troe, J.; Watson, R. T. *J. Phys. Chem. Ref. Data* **1980**, *9*, 295.
(27) Using the intensity 1×10^{13} cm^{-2} s^{-1} at 185 nm, and with kinetic and photochemical parameters from ref 26, the rate coefficients in eq 3 are $k_1 = 2 \times 10^{-7}$ s^{-1} and $k_2 = 1.4 \times 10^{-14}$ cm^3 s^{-1}.
(28) Ikeda, H.; Nakagawa, Y.; Toshima, M.; Furuta, S.; Zaima, S.; Yasuda, Y. *Appl. Surf. Sci.* **1997**, *117/118*, 109.
(29) Ikeda, H.; Nakagawa, Y.; Zaima, S.; Ishibashi, Y.; Yasuda, Y. *Jpn. J. Appl. Phys.* **1999**, *38*, 3422.
(30) Höfer, U. *Appl. Phys. A* **1996**, *63*, 533.
(31) Lide, D. R., Ed. *Handbook of Chemistry and Physics*, 3rd electronic ed.; CRC Press: Boca Raton, FL, 2000.
(32) Kemnitz, K.; Bhattacharyya, K.; Hicks, J. M.; Pinto, G. R.; Eisenthal, K. B. *Chem. Phys. Lett.* **1986**, *131*, 285.
(33) Hollering, R. W. J. *J. Opt. Soc. Am.* **1991**, *8*, 374.
(34) Hattori, T.; Aiba, T.; Iijima, E.; Okube, Y.; Nohira, H.; Tate, N.; Katayama, M. *Appl. Surf. Sci.* **1996**, *104/105*, 323.
(35) Teraishi, K.; Takaba, H.; Yamada, A.; Endou, A.; Gunji, I.; Chatterjee, A.; Kubo, M.; Miyamoto, A. *J. Chem. Phys.* **1998**, *109*, 1495.
(36) Luh, D.-A.; Miller, T.; Chiang, T.-C. *Phys. Rev. Lett.* **1997**, *79*, 3014.